

# Highly aligned narrow diameter chitosan electrospun nanofibers

Sajjad Haider · Yousef Al-Zeghayer · Fekri A. Ahmed Ali · Adnan Haider · Asif Mahmood · Waheed A. Al-Masry · Muhammad Imran · Muhammad Omer Aijaz

Received: 8 December 2012 / Accepted: 4 February 2013 / Published online: 6 March 2013  
© Springer Science+Business Media Dordrecht 2013

**Abstract** Random and highly aligned bead-free chitosan nanofibers (NFs) were successfully prepared via electrospinning by keeping the applied voltage (22 kV), flow rate (0.4 mL h<sup>-1</sup>), needle diameter (0.8 mm), and needle to collector distance (100 mm) constant while varying the solution concentration and collector rotation speed. No electrospinning was observed for lower solution concentrations, i.e., 1–3 wt% (w/v), whereas a decrease in the number and size of beads and microspheres, and bead-free NFs were obtained when the concentration of solution was increased from 4 to 6 wt%. Increase in the polymer concentration increased the solution viscosity (from 3.53 to 243 mPa s) and conductivity (from 29.80 to 192.00  $\mu\text{s cm}^{-1}$ ) to critical values, which led to beadless NFs. The optimized conditions (i.e., concentration of solution 6 wt%, applied electrical potential 22 kV, flow rate 0.4 mL h<sup>-1</sup>, needle diameter 0.8 mm, and needle to collector distance 100 mm) were further used for the alignment of chitosan NFs. The alignment of the NFs increased from 35.6

to 94.4 % and the diameter decreased from 163.9 to 137.4 nm as the rotation speed of the cylindrical collector drum was increased from 2.09 to 21.98 m s<sup>-1</sup>. The aligned and small diameter chitosan NFs might find potential applications in biomedical, environmental, solar fuel cell applications, etc. Several target devices and polymer systems in the literature have been used to obtain aligned NFs; however, almost no work has been reported on individual chitosan alignment.

**Keyword** Chitosan · Aligned · Nanofibers · Fine diameter

## Introduction

Electrospinning is a versatile technique for producing fibers with diameters between 10 and 200 nm and in some cases to micrometers [1]. Although the first ever patents on the electrical dispersion of fluids and fabrication of textile yarns from electrically dispersed fluids were registered in 1902 and 1934 [2], however true efforts using this technique started in the 1990s [3–5]. In 2011, a variety of organic and inorganic materials were not only successfully electrospun but were also used in industrial processes and products [6]. A typical electrospinning assembly consists of four components: (i) a pump, which holds a syringe containing polymer solution, and allows controlled outflow of polymer solution; (ii) a high voltage supply; (iii) a metallic capillary (needle), connected to syringe and a positive voltage; and (iv) a metallic collector (flat or rotation drum), connected to negative voltage [7]. During electrospinning, as the voltage is applied, the solution drop moves to the tip of the needle, the hemispherical shape of the droplet is destabilized by charges that accumulate on its surface, and it is converted to a Taylor's cone. At a critical voltage, the

---

S. Haider (✉) · F. A. Ahmed Ali · A. Mahmood · W. A. Al-Masry · M. Imran · M. O. Aijaz  
Department of Chemical Engineering,  
College of Engineering, King Saud University,  
P.O. Box 800, Riyadh 11421, Saudi Arabia  
e-mail: shaider@ksu.edu.sa

S. Haider  
e-mail: afridi\_phd@hotmail.com

Y. Al-Zeghayer  
Industrial Catalysis Research, College of Engineering,  
King Saud University,  
P.O. Box 800, Riyadh 11421, Saudi Arabia

A. Haider  
Department of Polymer Science,  
Kyungpook National University,  
1370 Sankyuk-dong, Buk-gu,  
Daegu 702-701, South Korea

electric forces overcome the surface tension on the droplet and a jet of ultra-fine fibers in the range of 10–200 nm or in some cases up 600 nm is produced from the tip of the Taylor's cone [5]. The bending instability of the electrified polymer jet during the stretching process causes the nonwoven NFs to be collected in a random orientation on the collector [8]. Owing to their fine diameter [9], large surface area per unit mass, high porosity, high gas permeability, and small interfibrous pore size [10], the randomly oriented NFs mats have found applications in filtration [11], wound dressing [12], drug delivery systems [13], and tissue engineering scaffolds [14]. More recently, researchers have shown that in addition to random orientation, NFs could also be electrospun in an aligned orientation. The aligned NFs showed enhanced mechanical, electrical, and optical properties when compared to randomly oriented NFs. Therefore these could find more advanced applications in solar cells, fuel cells [15–17], biomedical engineering for bioactive protein delivery [18], improve growth of nerve or muscle cells [19–21], wound dressing, and chemical and biological sensors [22]. A number of modified electrospinning assemblies were proposed [23–29] and used for the alignment of mainly synthetic polymers such as polycaprolactone (PCL), polyethylene oxide (PEO), poly(methyl methacrylate) (PMMA), polystyrene (PS), nylon-6, polyvinyl alcohol (PVA), polyacrylonitrile (PAN), and their blends with chitosan and chitosan derivatives (e.g., chitosan/PCL, chitosan/PEO, chitosan/PVA, and carboxymethyl chitosan/PVA [20, 21, 29, 30]). They showed excellent cellular biocompatibility which proves that chitosan and chitosan-based materials could be used in biomedical engineering [20, 21]. Chitosan, a cationic polysaccharide polymer, has been intensively studied owing to its abundance in nature, cheap availability, and potential biomedical applications [31]. However, there are almost no reports on its individual alignment. In some instances it has been blended with synthetic polymers [29, 30]. In this work we studied the alignment of chitosan NFs. We believe that our work will give researchers further insight into the utilization of chitosan NFs for more advanced applications.

## Materials and methods

### Materials

Medium molecular weight chitosan powder, trifluoroacetic acid ( $\text{CF}_3\text{COOH}$ , TFA), absolute ethanol ( $\text{C}_2\text{H}_5\text{OH}$ ), and acetone ( $\text{C}_3\text{H}_6\text{O}$ ) were purchased from Sigma-Aldrich, Alfa Aesar, Paneac Quimica SAU, and Scharlab S.L., respectively. All the chemicals were of analytical grade and were used without further purification. The basic electrospinning setup NANO-1A from Japan was used for the alignment of chitosan NFs.

### Electrospinning of solutions

Chitosan solutions at various concentrations (e.g., 1, 3, 4, 6, 8 wt% (w/v)) were prepared by dissolving chitosan in TFA using a sonicator bath (Branson 2510) at 55 °C for 90 min. After dissolution, the solutions were stirred for 15 min using magnetic stirrers (Cerastir 30539) and finally filtered through a mesh with 0.063 mm pore size to obtain homogeneous solutions and remove any undissolved particles. For electrospinning the solutions were added to a 5-mL plastic syringe of 10 mm diameter equipped with a stainless steel needle of 0.8 mm diameter. The syringe was placed in a syringe pump and the needle was connected to a high voltage supply, which could generate voltages of up to 30 kV. In this study, the applied voltage was 22 kV, flow rate was 0.4 mL h<sup>-1</sup>, the distance between needle tip and collector was 100 mm, and the speed of the cylindrical collector was changed from 2.09 to 21.98 m s<sup>-1</sup>. After electrospinning the NFs mats were removed from the rotating drum, dried in a vacuum oven (DP63, Yamata Scientific Co. Ltd) at 60 °C and at -0.1 MPa, and then stored in a desiccator until characterization.

### Morphology of NFs

Morphologies of the aligned NFs samples were studied by field emission scanning electron microscopy (FE-SEM) (JSM-7600F). To study the surface morphology of the electrospun NFs via FE-SEM, NFs samples were fixed onto a holder with the aid of carbon tape and then placed in the sputtering machine for platinum coating (to increase their electrical conductivity). After platinum coating the electrospun NFs were examined by FE-SEM under high vacuum.

### Measurement of diameter and alignment angle

To measure the diameter and alignment angle of the NFs, Adobe Photoshop software was used. Approximately 250 NFs were randomly selected and their diameter and angle of alignment were measured. Photoshop was used to measure the diameter which was numerically converted using the scale bar on the FE-SEM micrograph. The alignment angle was considered as a reference angle (zero angle) and all deviations were measured relative to that angle.

## Results and discussion

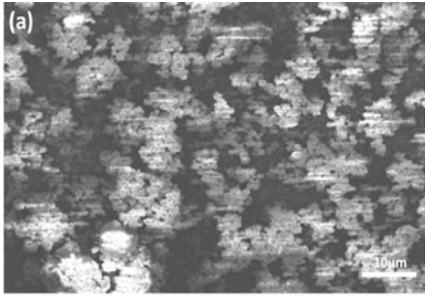
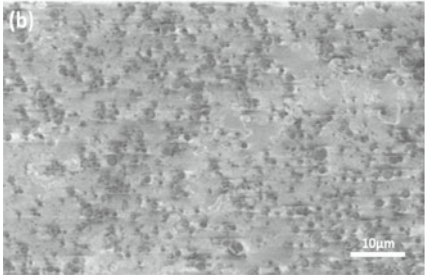
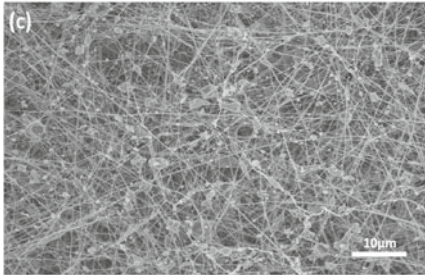
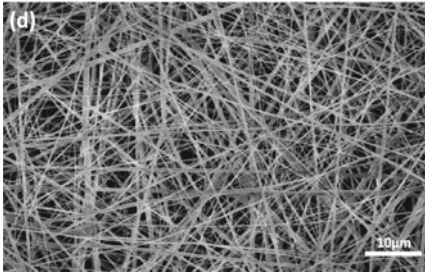
### Effect of solution concentration

Although electrospinning is an efficient method for producing continuous polymer NFs, there are a number of variables that can affect NFs morphologies. In order to control NF morphologies, one must understand the electrospinning

process and the parameters that influence it, such as polymer concentration, solution conductivities, needle inner diameter, feed rate, needle tip to collector distance, and electric field voltage. All these parameters significantly affect the

spinability and quality of the polymer solution. Table 1 shows the effects of various solution concentrations (in the range of 1 to 6 wt%) and their resulting viscosity and conductivity on the morphology and average

**Table 1** Relationship between chitosan concentration and morphology of NFs at constant flow rate, needle diameter, applied voltage, and needle tip to collector distance

Conc. (wt%)	Viscosity (mPa s)	Conductivity (μs/cm)	Fiber form	Morphology scale bar (1μm)
1	3.53	29.80	Droplets	
3	22.90	69.00	Droplets	
4	58.50	104.00	Beaded NFs	
6	243.00	192.00	Continuous bead-less NFs	

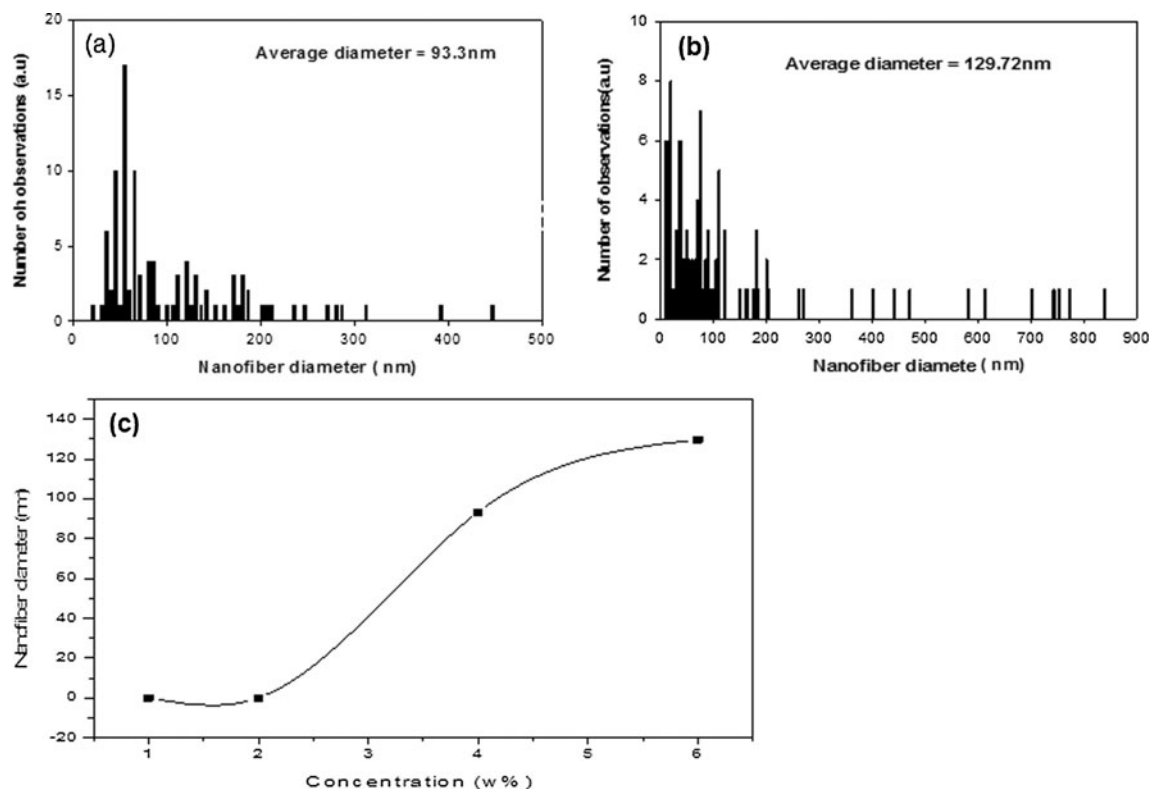


**Fig. 1** Effect of chitosan solution concentration on the diameter distribution of NFs at constant applied voltage, flow rate, tip to collector distance, and needle diameter: **a** 4 wt% histogram, **b** 6 wt% histogram, **c** sigma plot of the same

diameter of the NFs prepared from a chitosan–TFA solution. We observed that 1–3 % did not show electrospinning and only droplets (Table 1, insets a, b) were obtained; the process under these conditions is the classic electro spraying rather than electrospinning. The formation of these droplets is attributed to the insufficient molecular chain entanglements, low surface tension, and low conductivities of the polymer solution, which allowed the breakup of the electrically driven jet into droplets [32, 33]. Stable jet formation is not only effected by solution concentration but also by conductivities. Researchers sometime use salt to make solutions more conductive to facilitate jet drawing and obtain well-defined NFs [34]. Increasing the concentration of solution from 3 to 4 wt% changed the morphology of electrospun NFs membrane from droplets to beaded NFs (Table 1, inset c). This change in morphology might be linked to the increased molecular entanglement [35] and conductivities, which prevented jet breaking. However, the presence of the beads showed that the chain entanglements are still not enough to make the jet completely stable [32, 33]. Further increase in the solution concentration (from 4 to 6 wt%) not only led to the disappearance of beads (Table 1, inset d) but also increased the average diameter from 93.3 to 129.72 nm (Fig. 1a–c). This means that there is a

higher amount of polymer chain entanglement in the solution, which led to a slight decrease in stretching but to a stable charged jet formation [36]. The stable jet formation is an indication that viscosity, conductivity, and surface tension of the solution reached a critical value, which avoided the breakup of polymer drop at the needle tip (if there is breakup, electro spray occurs) [37]. At 8 wt% solution concentration no electrospinning was observed as the solution was very viscous (semi-solid), which resulted in the drying of the drop at the needle tip. The optimum conditions for the preparation of the chitosan NFs mats are given in Table 2.

**Table 2** Optimal parameters for the fabrication of random and aligned NFs

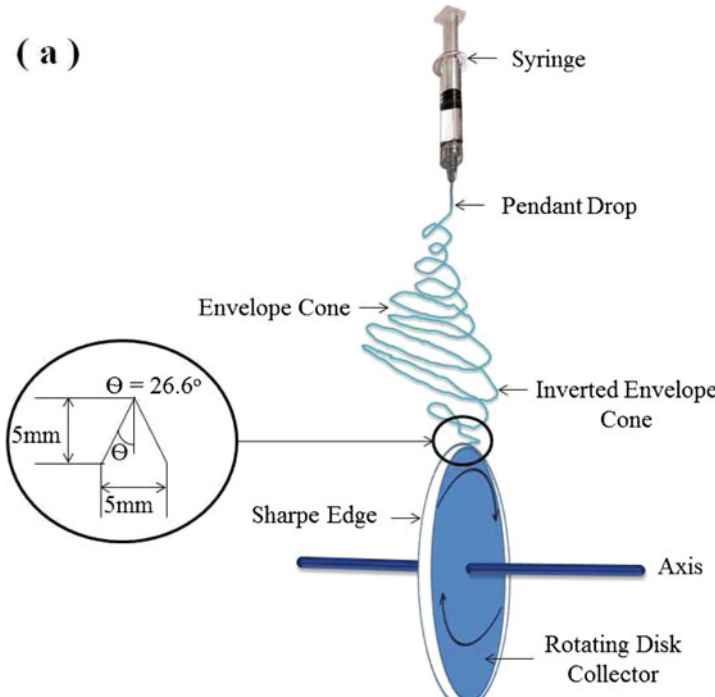
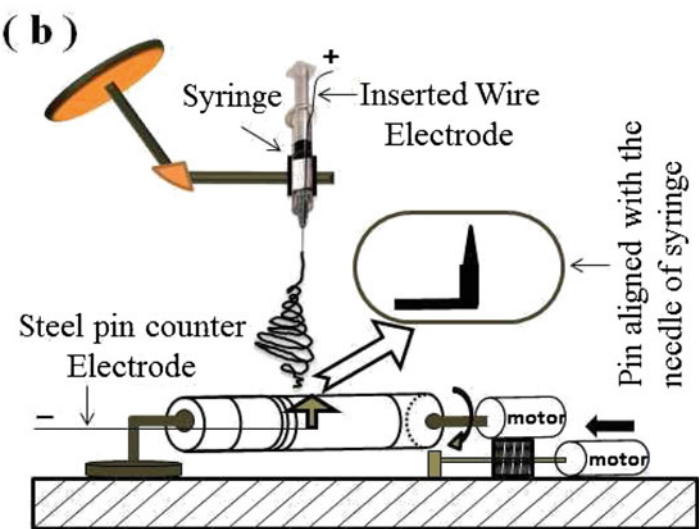
Parameter	Optimized value
Concentration	6 wt%
Flow rate	0.8 mL h <sup>-1</sup>
Voltage applied	22 kV
Needle diameter	0.8 mm
Needle to collector distance	100 mm
Viscosity	243.00 mPa s
Solution conductivity	192.00 $\mu$ s cm <sup>-1</sup>

Collector design and alignment of NFs

Table 3 shows the schematics of a variety of collector designs used for aligning NFs during electrospinning. Theron et al. [19] combined an electrostatic field-assisted assembly with electrospinning process to align individual PEO NFs by replacing the conventional collector with a grounded wheel-like bobbin (Table 3, inset a). The bobbin wound the continuously spinning NFs of 100–300 nm in diameter and hundreds of

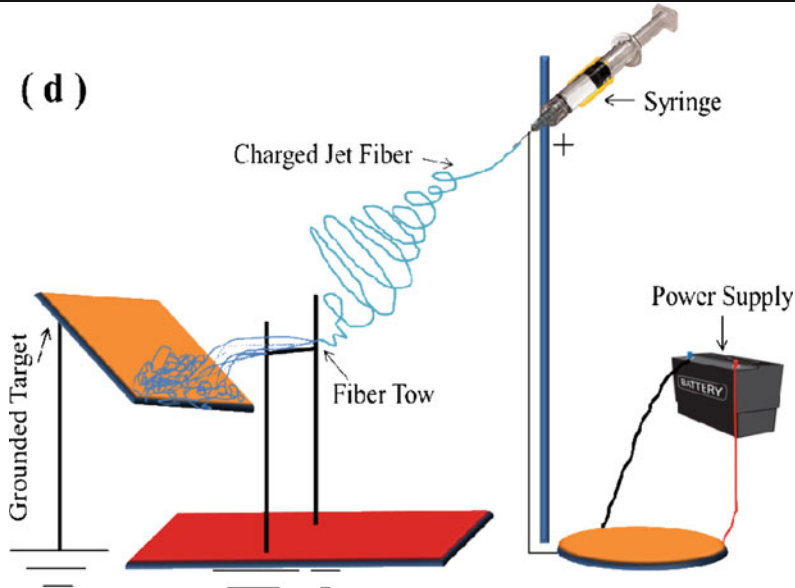
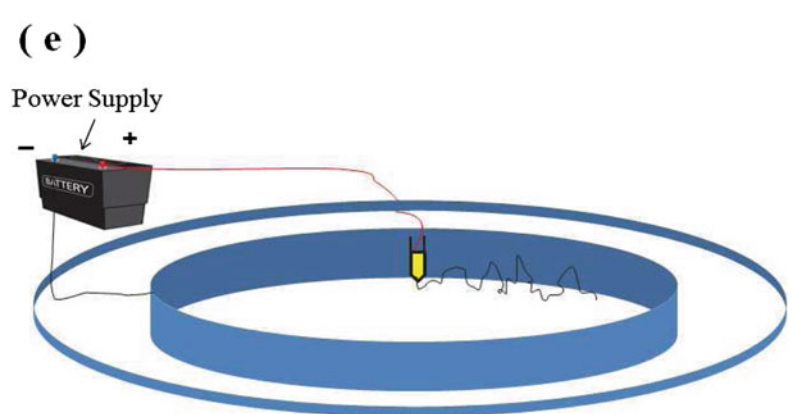
microns in length at its tip-like edge. The technique was effective in assembling NFs in parallel arrays with controlled average fiber separation [19] but lacked in the production of large quantity samples. Sundaray et al. used a conventional electrospinning assembly with a flexible plastic film substrate on a rotating drum collector (Table 3, inset b). They obtained long aligned parallel and criss-cross patterns of polymer fibers with a very narrow range but increased diameters (i.e., 1–10 μm). The obtained fibers were several centimeters long

**Table 3** Various designs of the target apparatus used for the alignment of NFs

Polymer	Technique	Schematic	Ref.
PEO	Tip-like edge	 <p>(a)</p>	[19]
PMMA/ PS	Plastic Film on Rotating Drum	 <p>(b)</p>	[23]

All the schematics were redrawn by the author

Table 3 (continued)

Nylon-6	Multiple Parallel Copper Electrodes Collector	(c)	[24]
			
PVA	Dual Vertical Wire Collector	(d)	[25]
			
PAN	Modified Rotating Jet	(e)	[26]
			

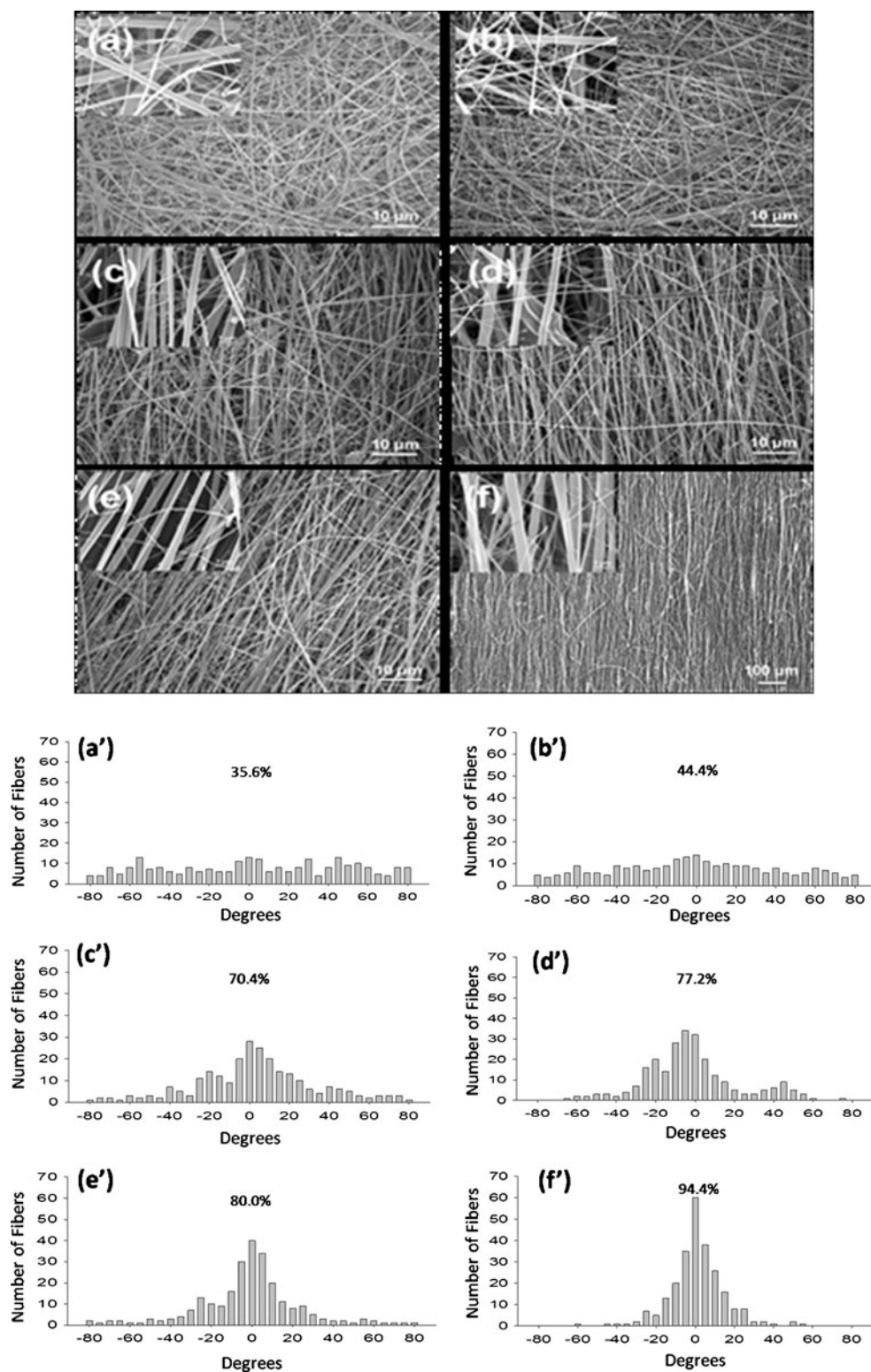
with fiber to fiber spacing of 5–100  $\mu\text{m}$  [23]. Katta et al. [24] replaced the conventional drum collector with copper wires collector. The copper wires were spaced evenly in the form of a circular drum (Table 3, inset c). An aligned fiber sheet of approximately 1 cm width was obtained with this technique. Alignment of the NFs is driven by electrostatic interactions allowing the charged NFs to stretch and span across the gap

between the wires and to form axially aligned arrays over large areas [24]. Chuangchote et al. used a dual vertical wire technique for the fabrication of uniaxially aligned PVA fibers (Table 3, inset d). They placed two stainless steel wires vertically parallel between a charged needle and a grounded collector plate and obtained simultaneously aligned NFs (in the range of 340 to 350 nm) between the parallel vertical wires

**Table 3** (continued)

PCL	Inclined Gap Collector	<p><b>(f)</b></p>	[27]
Chitosan/ PVA	Rotating rectangular metal frame wire, metal wire around nanoconductive drum, rotating points and wire bars	<p><b>(g)</b></p>	[28]
Chitosan	High speed rotation	<p><b>(h)</b></p>	Present work

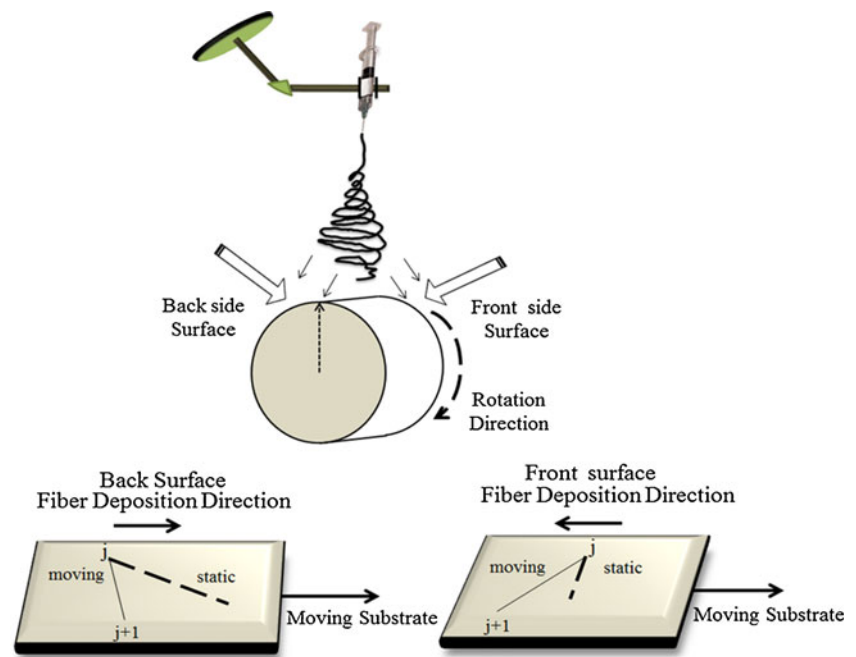
**Fig. 2** FE-SEM micrographs (a–f) and the corresponding histograms (a'–f') of the chitosan NFs alignment at optimized electrospinning conditions by controlling the collector (cylindrical drum) rotation speed:  $2.09 \text{ m s}^{-1}$  (a, a'),  $5.20 \text{ m s}^{-1}$  (b, b'),  $9.42 \text{ m s}^{-1}$  (c, c'),  $13.60 \text{ m s}^{-1}$  (d, d'),  $17.79 \text{ m s}^{-1}$  (e, e'),  $21.98 \text{ m s}^{-1}$  (f, f')



and randomly aligned NFs on the collector plate. The technique was, however, successful in obtaining aligned NFs for a very short time of 30 s [25]. More recently Khamforoush and Mahjob [26] designed a modified rotating jet technique (Table 3, inset e) to increase the amount and degree of alignment of the PAN nanofibers. The cylindrical collector of the

rotating jet method (RJM) was replaced by two metallic concentric hollow cylinders. This significantly improved the degree of alignment by more than double and increased the average production rate by 41 % compared with that of the RJM [26]. Park and Yang [27] introduced inclined gap collectors (conductive strips configured horizontally and

**Scheme 1** Mechanism of the NF stretching and alignment. The diagrams are restructured from ref. [39]



vertically) (Table 3, inset f) and obtained well-aligned PCL NFs with diameters ranging from 500 to 700 nm for maximum duration of 50 s. The electrospun NFs were sequentially suspended across the edges of strips in a well-aligned and regularly distributed manner [27]. Afifi et al. [28] studied the alignment of chitosan/PVA blend using four different designs of collector (i.e., rotating rectangular metal frame wire, metal wire around nanoconductive drum, rotation drum points, and wire bars; Table 3, inset g) and rotating pointed drum for poly (L-lactide acid) (PLLA). Improved alignment (i.e., 90 % alignment for chitosan/PVA [28] and 60 % for PLLA [37]) was obtained with the rotating pointed drum. However, most of these newly designed collectors were unable to collect enough sample to be used in further analysis. The reasons were that in some cases the collector areas was too small (tip-like edge and rotation pointed), whereas in others the NFs

deviated from the axis of aligned nanofiber with increase in time (dual vertical wire technique and inclined gap collectors). Besides, the diameter of the NFs was also very large. We have successfully produced highly aligned individual chitosan nanofibers with fine diameter by controlling the drum rotation speed (Table 3, inset h).

#### Chitosan NF alignment

In an effort to align the fibers, the drum rotation speed, which is a key parameter, needs to be controlled. Figure 2 shows the alignment of chitosan NFs at optimized electrospinning conditions (Table 2) using controlled rotation speed of the cylindrical drum. When the rotation speed was  $2.09 \text{ m s}^{-1}$  (Fig. 2a, a'; 35.6 % alignment) and  $5.20 \text{ m s}^{-1}$  (Fig. 2b, b'; 44.4 % alignment) the fiber was deposited randomly. This random disposition of the fiber onto the rotating drum could be attributed to the high velocity of the electrified jets and high-speed instabilities [38]. The fibers started to align as the rotation speed reached  $9.42 \text{ m s}^{-1}$  (Fig. 2c, c'; 70.4 % alignment) and improved alignment with some misaligned NFs was observed at a rotation speed of  $13.60 \text{ m s}^{-1}$  (Fig. 2d, d'; 77.2 % alignment) and  $17.79 \text{ m s}^{-1}$  (Fig. 2e, e'; 80.0 % alignment). The misalignment of NFs might occur because when jets deposit on the frontside surface of the rotating drum (Scheme 1), the fibers are mechanically pulled and stretched, leading to alignment; on the contrary, deposition of the fibers jets on the backside surface of the rotating drum results in looping and poor orientation. Uniformly aligned chitosan NFs were obtained when the rotation speed of the drum was further increased to  $21.98 \text{ m s}^{-1}$  (Fig. 2f, f'; 94.4 % alignment). This

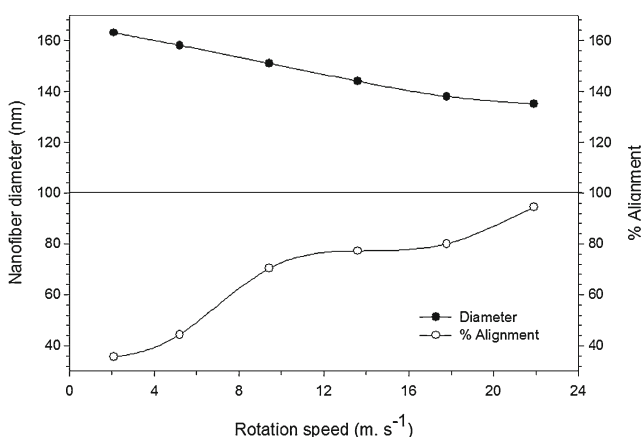


**Fig. 3** Effects of rotation speed on alignment and diameter of the chitosan NFs

alignment of chitosan NFs might be the result of the increased jet stability owing to the matching of velocities of the jets and drum rotation, and decrease in the looping owing to increase in the number of NFs striking on the front of the drum [39].

#### Effect of rotation speed on NF diameter

Figure 3 shows the effect of rotation speed on the diameter of chitosan nanofibers. The diameter of the NFs continuously decreased from 163.9 to 137.4 nm as the speed of the rotating cylindrical drum increased from 2.09 to 21.98 m s<sup>-1</sup>. This decrease in diameter with increase in rotation speed might be due to the fact that when a collector is moving, after the initial deposition of fiber particle, the incoming fiber particle (j+1) and the particles in flight which are connected to the deposited particle experience additional mechanical forces. This mechanical force not only caused fiber stretching, i.e., decreased the diameter, but also aligned the fibers (Scheme 1, Fig. 3). The stretching and alignment depend on the orientation of the directions of NF deposition and surface motion. When the jet is being deposited in the preferential direction (frontside), the jet will receive not only additional stretching but will be more aligned (black line) with respect to the surface motion direction compared to the case of a stationary substrate (dotted line). The NF stretching and alignment effects will be reversed if the preferential jet deposition direction coincides with the substrate motion direction (backside) [39]. The stretching as well as alignment could be improved by increasing the substrate motion velocity which is in agreement with our results [37].

#### Conclusions

Aligned and bead-free individual chitosan NFs were successfully prepared via electrospinning by controlling solution concentration and collector rotation speed, while keeping the applied voltage, flow rate, needle diameter, and needle to collector distance constant. No electrospinning was observed for lower solution concentration samples, i.e., 1–3 wt%, whereas a decrease in the number and size of the beads and microspheres, and bead-free NFs were obtained when the concentration of solution was increased to 6 wt%. Increase in the polymer concentration increased the solution viscosity (from 3.53 to 243 MPa s) and conductivity (from 29.80 to 192.00  $\mu\text{s cm}^{-1}$ ) to critical values, which led to beadless NFs. The optimized conditions were further used to align individual chitosan NFs. The alignment of the NFs increased from 35.6 to 94.4 % and the diameter decreased from 163.9 to 137.4 nm as the rotation speed of the cylindrical collector drum increased from 2.09 to 21.98 m s<sup>-1</sup>. The aligned and small

diameter chitosan NFs might find potential applications in solar cells, fuel cells, biomedical engineering for bioactive protein delivery, improve growth of nerve or muscle cells, wound dressing, and chemical and biological sensors, etc.

**Acknowledgments** Financial support from the National Plan for Science and Technology, King Saud University, Saudi Arabia under the grant 09-NANO869-02 is greatly acknowledged.

#### References

- Greiner A, Wendorff JH (2007) Electrospinning: a fascinating method for the preparation of ultrathin fibers. *Angew Chem Int Ed* 46:5670–5703
- Cooley JF (1902) Apparatus for electrically dispersing fluids. US Patent 692,631
- Formhals A (1934) Process and apparatus for preparing artificial threads. US Patent 1,975,504
- Doshi J, Reneker DH (1995) Electrospinning process and applications of electrospun fibers. *J Electrostat* 35:151–160
- Reneker DH, Chun I (1996) Nanometre diameter fibres of polymer, produced by electrospinning. *Nanotechnology* 7:216–223
- Jian F, Xungai W, Tong L (2011) Functional applications of electrospun nanofibers. In: Lin T (ed) *Nanofibers: production, properties and functional applications*. InTech, Rijeka, pp 287–326
- Li D, Xia Y (2004) Electrospinning of nanofibers: reinventing the wheel? *Adv Mater* 16:1151–1170
- Usman A, Yaqiong Z, Xungai W, Tong L (2011) Electrospinning of continuous nanofiber bundles and twisted nanofiber yarns. In: Lin T (ed) *Nanofibers: production, properties and functional applications*. InTech, Rijeka, pp 420–427
- Ohkawa K, Cha D, Kim H, Nishida A, Yamamoto H (2004) Electrospinning of chitosan. *Macromol Rapid Commun* 25:1600–1605
- Buchko CJ, Chen LC, Shen Y, Martin DC (1999) Processing and microstructural characterization of porous biocompatible protein polymer thin films. *Polymer* 40:7397–7407
- Qin XH, Wang SY (2006) Filtration properties of electrospinning nanofibers. *J Appl Polymer Sci* 102:1285–1290
- Zahedia P, Rezaeiana I, Ranaei-Siadatb SO, Jafaria SH, Supaphol PA (2010) Review on wound dressings with an emphasis on electrospun nanofibrous polymeric bandages. *Polym Adv Technol* 21:77–95
- Yu DG, Zhu LM, White K, White CB (2009) Electrospun nanofiber-based drug delivery systems. *Health* 1:67–75
- Pham QP, Sharma U, Mikos AG (2006) Electrospinning of polymeric nanofibers for tissue engineering applications: a review. *Tissue Eng* 12:1197–1211
- Shim HS, Kim JW, Kim WB (2009) Fabrication and optical properties of conjugated polymer composited multi-arrays of TiO<sub>2</sub> nanowires via sequential electrospinning. *J Nanosci Nanotechnol* 9:4721–4726
- Liao IC, Chew SY, Leong KW (2006) Aligned core-shell Nanofibers delivering bioactive proteins. *Nanomedicine (Lond)* 1:465–471
- Tamura T, Kawakami H (2010) Aligned electrospun nanofiber composite membranes for fuel cell electrolytes. *Nano Lett* 10:1324–1328
- Meng ZX, Wang YS, Ma C, Zheng W, Li L, Zheng YF (2010) Electrospinning of PLGA/gelatin randomly-oriented and aligned nanofibers as potential scaffold in tissue engineering. *Mater Sci Eng C* 30:1204–1210

19. Theron A, Zussman E, Yarin AL (2001) Electrostatic field-assisted alignment of electrospun nanofibers. *Nanotechnology* 12:384–390
20. Bhattarai N, Edmondson D, Veisoh O, Matsen FA, Zhang M (2005) Electrospun chitosan-based nanofibers and their cellular compatibility. *Biomaterials* 26:6176–6184
21. Cooper A, Jana S, Bhattarai N, Zhang M (2010) Aligned chitosan-based nanofibers for enhanced myogenesis. *J Mater Chem* 20:8904–8911
22. NASA Langley's (2008) Highly aligned electrospun fibers and mats. NP-2008-04-77-LaRC:1(4). [http://technologygateway.nasa.gov/docs/TOA\\_LARC04\\_AlignElectroNano\\_16web.pdf](http://technologygateway.nasa.gov/docs/TOA_LARC04_AlignElectroNano_16web.pdf). Accessed 11 Aug 2012
23. Sundaray B, Subramanian V, Natarajan TS, Xiang RZ, Chang CC, Fann WS (2004) Electrospinning of continuous aligned polymer fibers. *Appl Phys Lett* 84:1222–1224
24. Katta P, Alessandro M, Ramsier RD, Chase GG (2004) Continuous electrospinning of aligned polymer nanofibers onto a wire drum collector. *Nano Lett* 4:2215–2218
25. Chuangchote S, Supaphol P (2006) Fabrication of aligned poly(vinyl alcohol) nanofibers by electrospinning. *J Nanosci Nanotechnol* 6:125–129
26. Khamfroush M, Mahjob M (2011) Modification of the rotating jet method to generate highly aligned electrospun nanofibers. *Mater Lett* 65:453–455
27. Park SH, Yang DY (2011) Fabrication of aligned electrospun nanofibers by inclined gap method. *J Appl Polymer Sci* 120:1800–1807
28. Affi AM, Yamamoto M, Yamane H, Kimura Y, Salmawy AE, Nakano S (2011) Electrospinning and characterization of aligned nanofibers from chitosan/polyvinyl alcohol mixtures: comparison of several target devices newly designed. *Sen-I Gakkaishi* 67:103–108
29. Mincheva R, Manolova N, Rashkov I (2007) Bicomponent aligned nanofibers of N-carboxyethyl chitosan and poly(vinyl alcohol). *Eur Polym J* 43:2809–2818
30. Haider S, Park SY (2009) Preparation of the electrospun chitosan nanofibers and their applications to the adsorption of Cu(II) and Pb(II) ions from an aqueous solution. *J Membr Sci* 328:90–96
31. Taylor G (1969) Electrically driven jets. *Proc R Soc Lond A* 313:453–475
32. Ramakrishna S, Fujihara K, Teo WE, Lim TC, Ma Z (2005) Introduction to electrospinning and nanofibers. World Scientific, Singapore
33. Liu Y, He JH, Yu JY, Zeng HM (2008) Controlling numbers and sizes of beads in electrospun nanofibers. *Polym Int* 57:632–636
34. Kriegel C, Kit KM, McClements DJ, Weiss J (2009) Electrospinning of chitosan–poly(ethylene oxide) blend nanofibers in the presence of micellar surfactant solutions. *Polymer* 50:189–200
35. Homayoni H, Abdolkarim S, Ravandi H, Valizadeh M (2009) Electrospinning of chitosan nanofibers: processing optimization. *Carbohydr Polym* 77:656–661
36. Rutledge GC, Warner SB, Ugbohue SC (2001) Electrostatic spinning and properties of ultrafine fibres. National Textile Centre Annual Report. <http://www.ntcresearch.org/pdf-rpts/AnRp04/M01-MD22-A4.pdf>. Accessed 22 Feb 2013
37. Affi AM, Nakajima H, Yamane H, Kimura Y, Nakano S (2009) Fabrication of aligned poly(L-lactide) fibers by electrospinning and drawing. *Macromol Mater Eng* 294:658–665
38. Teo WE, Inai R, Ramakrishna S (2011) Technological advances in electrospinning of nanofibers. *Sci Technol Adv Mater* 12:013002
39. Liu L (2006) Studies on deposition and alignment of electrospun nanofiber assemblies. University of Nebraska, Lincoln. <http://digitalcommons.unl.edu/dissertations/AAI3296165>. Accessed 11 Aug 2012